Developmental Biology **248,** 107–117 (2002)
doi:10.1006/dbio.2002.0709

in Eye and Tectum Development

Atsuo Kawahara,*[,1] Chi-Bin Chien,† and Igor B. Dawid*[,1]

**Laboratory of Molecular Genetics, National Institute of Child Health and Human Development, National Institutes of Health, Bethesda, Maryland 20892; and †Department of Neurobiology and Anatomy, University of Utah Medical Center, 50 North Medical Drive, Salt Lake City, Utah 84132*

The homeobox gene *mbx* is first activated at the end of gastrulation in zebrafish in the presumptive forebrain and midbrain region. During somitogenesis stages, the anterior expression of *mbx*, which partly overlaps the future eye field, gradually decreases, while midbrain expression intensifies and becomes restricted to the presumptive tectum. Knockdown of *mbx* expression by morpholino antisense oligonucleotides (mbx-MO) leads to a reduction in the size of the eyes and tectum. Expression domains of *rx1* and *pax6* in the eye field and of *mab21l2* in the eye field and tectum anlage were reduced in size in mbx-MO-injected embryos by somitogenesis stages. Further, induction of *islet1* and *lim3* expression in the eye at 2 days postfertilization (dpf) was suppressed in mbx-MO-injected embryos. In mbx-MO-injected embryos at 2–5 dpf, the lamination of the eye was disorganized and the number of retinal axons was substantially reduced, but the few remaining axons navigated appropriately to the contralateral tectum. A chimeric protein composed of the Mbx DNA-binding domain and the VP16 activation domain affected eye and tectum development similarly to mbx-MO knockdown, suggesting that Mbx acts as a transcriptional repressor in the zebrafish embryo. Based on these data, we propose that the *mbx* homeobox gene is required for the development of the eyes and tectum.

***Key Words: mbx*; homeobox gene; eye; tectum; midbrain–hindbrain boundary; morpholino.**

INTRODUCTION

Initial specification of the brain during early neurogenesis results in subdivision of the neural plate into the forebrain, midbrain, hindbrain, and spinal cord along the anterior–posterior axis. Among the various factors involved in nervous system patterning, homeobox genes are particularly prominent. One of the earliest regionalization events in the neuroectoderm during gastrulation is a division into presumptive hindbrain vs mid/forebrain through the expression of the *Gbx2* and *Otx2* genes (Wurst and Bally-Cuif, 2001). The *Otx2/Gbx2* boundary evolves into the midbrain–hindbrain boundary (MHB), which constitutes a major organizing center that controls the development of the surrounding regions of the brain (Rhinn and Brand, 2001; Wurst and Bally-Cuif, 2001). Within the forebrain, the eye field is distinguished from an early stage onward by the highly specific expression of homeobox genes that control its specification. In both zebrafish and mice, the expression of *Pax6* is first detected in the optic primordium and later in all cells of the prospective retina and lens (Puschel *et al.*, 1992; Walther *et al.*, 1991). In *Drosophila* and the mouse, the *Pax6* gene is required for eye formation, being affected in the *eyeless* and the *small eye* mutations, respectively (Quiring *et al.*, 1994; Ton *et al.*, 1992). A homeobox gene from a different class, *Rx1*, is likewise expressed specifically in the vertebrate eye field during early development, and overexpression and ablation studies have shown that *Rx1* is required for eye formation (Andreazzoli *et al.*, 1999; Chuang and Raymond, 2001; Mathers *et al.*, 1997; Zhang *et al.*, 2000).

Beyond specification of the eye field, additional regionalization events linked to the specific expression of genes encoding homeodomain proteins and other transcription factors occur during the development of the vertebrate fore- and midbrain (Appel, 2000; Rubenstein *et al.*, 1998). The MHB organizing center affects the development of the midbrain (Wurst and Bally-Cuif, 2001). The *Engrailed 1, 2* (*En1, 2*) and *Pax2, 5* genes are predominantly expressed in

[1] To whom correspondence should be addressed. Fax: (301) 496-0243. E-mail: kawahara@exchange.nih.gov or idawid@nih.gov.

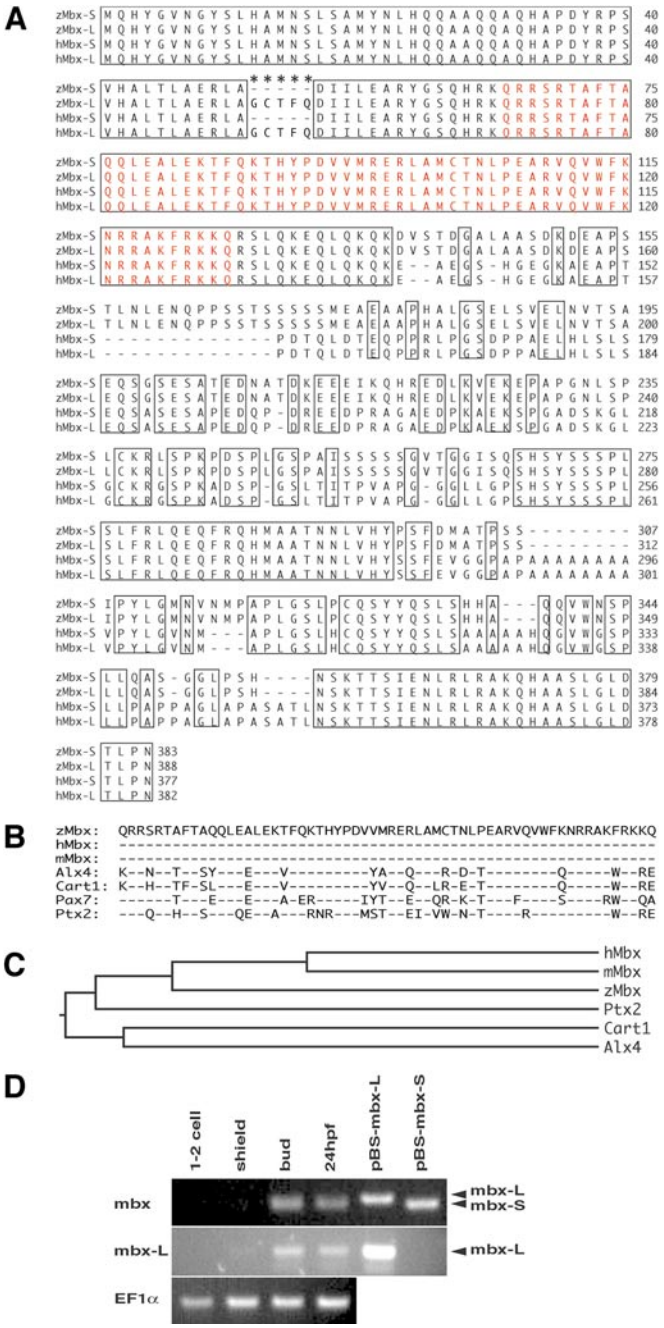

FIG. 1. Molecular analysis of *mbx*. (A) Predicted protein sequence of Mbx. Identical amino acids between zebrafish (z) and human (h) Mbx are boxed, and the homeodomain is indicated by red letters. Asterisks show the five amino acids specific to the long form. (B) Sequence alignment of homeodomains of Mbx with Alx4 (Qu *et al.*, 1997), Cart1 (Zhao *et al.*, 1993), Pax7 (Jostes *et al.*, 1990), and Ptx2 (Arakawa *et al.*, 1998); hyphens indicate identity. (C) Phylogenetic tree, based on full-length amino acid sequences, including mouse Mbx (Miyamoto *et al.*, 2002). (D) RT-PCR analysis of *mbx-S* and *mbx-L* expression in zebrafish at the indicated stages. pBS-mbx-S and pBS-mbx-L are positive control plasmids for the short and long splicing form, respectively. In the upper panel, common primers for *mbx-S* and *mbx-L* genes were used, while long form-specific primers were used in the second panel. The third panel represents EF1α loading controls.

the MHB and contribute to the development of the tectal region as well as the MHB (Schwarz *et al.*, 1997; Urbanek *et al.*, 1997; Wurst *et al.*, 1994). In fact, *Pax2/Pax5* double knockout mice display severe defects in both midbrain and cerebellum (Schwarz *et al.*, 1997; Urbanek *et al.*, 1997). Consistent with these findings, the zebrafish *no isthmus* (*noi*) mutant, in which *pax2.1* is disrupted, has severe defects in the midbrain, MHB, and cerebellum (Lun and Brand, 1998). In chicken, misexpression of *Pax3*, *Pax7*, or *Pax2* in the diencephalon induces an ectopic tectum (Matsunaga *et al.*, 2001), suggesting that these genes have a role in tectum development. Consistent with the wide expression of *Pax3* and *Pax7* in the brain (Goulding *et al.*, 1991; Jostes *et al.*, 1990; Seo *et al.*, 1998), mice doubly mutant for these genes exhibit extensive exencephaly and spina bifida (Mansouri and Gruss, 1998). However, no factor has been described so far that is expressed predominantly in the tectum at early neurogenesis stages and thus could be a likely candidate regulator of tectal development. Here, we describe a homeobox gene, *mbx*, which is first expressed during early somitogenesis in two domains, one at the anterior edge of the neural plate partly overlapping the future eye field, and a second, more intense domain in the presumptive midbrain. While *mbx* expression in the anterior neural plate gradually disappears, its midbrain expression is maintained and becomes concentrated in the tectum by 26 h postfertilization (hpf). Based on results using an antisense approach, we propose that *mbx* function is involved in anterior brain development, including the formation of the eyes and tectum.

MATERIALS AND METHODS

Gene Isolation and Manipulations

We found *mbx* as a previously unreported homeobox gene in the zebrafish EST database (Accession No. AI877798 in GenBank) and in the human genome sequence. RACE was performed starting with this sequence information and revealed two splice forms for *mbx* genes in both species. The *mbx* genes were then isolated from a 24-hpf zebrafish and a human fetus cDNA library by using the following oligonucleotide primers: z-mbx-F, 5′-CGGGATCCGGACATCTGGGAAATACTTCGAGC-3′; z-mbx-R, 5′-GCTCTAGATGACTAAATCATCAATGCTG-3′; h-mbx-F, 5′-CGGGATCCGCCGCCATGCAGCACTACGGGGTG-3′; and h-mbx-R, 5′-GCTCTAGATCAGTTGGGCAGCGTATCGAG-3′. After *Bam*HI and *Xba*I restriction enzyme digestion, the resulting DNA fragments were inserted into *Bam*HI–*Xba*I-cleaved pCS2+ vector. The GenBank Accession Nos. are *z-mbx-L*, AF398525; *z-mbx-S*, AF398526; h-mbx-S, AF398527; and h-mbx-L, AF398528. We have reported the sequence of mouse *mbx* elsewhere (Miyamoto *et al.*, 2002).

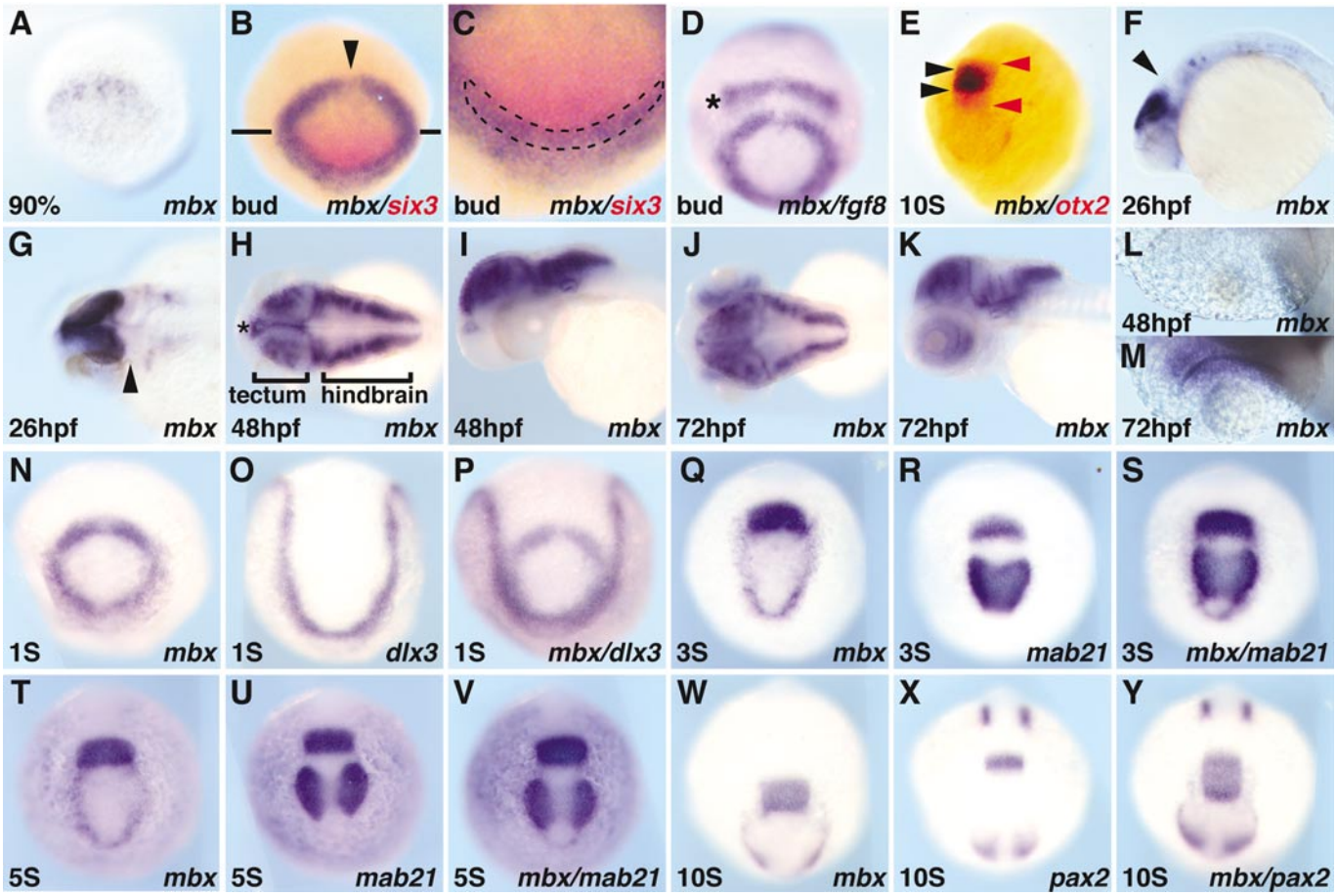

FIG. 2. Expression pattern of *mbx*. Whole-mount *in situ* hybridization with probes shown at bottom right of each panel. Stages are indicated at bottom left, with % referring to epiboly, S to somite, and hpf to hours postfertilization. Approximate times after fertilization are 90% epiboly (9 hpf), bud (10 hpf), 1S (10.3 hpf), 3S (11 hpf), 5S (11.6 hpf), and 10S (14 hpf). Lateral view, anterior is left (F, I, K); anterior view, dorsal is up (A–E, N–Y); dorsal view, anterior is left (G, H, J, L, M). The expression of *mbx* is not detected by midgastrulation, but arises in the anterior neural ectoderm at late gastrula (A). At bud stage (B–D), *mbx* is expressed in a ring with a midline gap (B, arrowhead), and partly overlaps the *six3* expression domain (C, overlap marked by dashed line). There is a gap between the *fgf8* (D; asterisk) and *mbx* expression domains, while anterior *mbx* expression partly overlaps with *dlx3* (N–P). During somitogenesis (N, Q, T, W), the posterior *mbx* domain fuses at the midline and increases in intensity, while the anterior domain elongates and then fades. Before fading, the anterior *mbx* domain overlaps with the eye field marked by *mab21l2* (Q–S). The posterior stripe corresponds to the prospective tectum; this stripe (E; black arrowheads) is included in the *otx2* expression domain (E; red arrowheads), overlaps with the posterior *mab21l2* domain (Q–V), and is located just anterior of *pax2.1* (W–Y). By 26 hpf, *mbx* is predominantly expressed in the tectum, with weak staining detected in some hindbrain and spinal neurons; *mbx* is excluded from the midbrain–hindbrain boundary (MHB) (F, G; arrowhead). (H–M) Expression pattern of *mbx* during hatching period; *mbx* is expressed in diencephalon (H: asterisk), tectum, otic vesicle, and rhombomeres at 48 and 72 hpf, while the retina is stained at 72 hpf, but not at 48 hpf (L, M).

For construction of Mbx-GFP, the 5′-UTR and N-terminal domain (amino acids 1–172) of *z-mbx-S*, which contains the sequence complementary to mbx morpholinos, was fused to the enhanced green fluorescent protein gene (EGFP: amino acids 1–257) containing the nuclear localization signal of SV40. For construction of VP16-Mbx and ENG-Mbx, the VP16 activation domain (amino acids 410–489) and the Engrailed repressor domain (amino acids 1–298) (Kawahara *et al.*, 2000) were connected to the C-terminal domain of *z-mbx-S* containing the homeodomain (amino acids 52–383), which is conserved between *z-mbx-S* and *z-mbx-L*.

Zebrafish Mutants and Whole-Mount in Situ Hybridization

The *tt250* allele of *chordino* (*din*), *tc300* allele of *swirl* (*swr*), *ti282a* allele of *acerebellar* (*ace*), *tu29a* allele of *no isthmus* (*noi*), and *headless* (*hdl*) were used. Whole-mount *in situ* hybridization was performed as described, using the combination of digoxigenin-labeled antisense RNA probe and α-digoxigenin alkaline phosphatase-conjugated antibody (Roche) (Kawahara *et al.*, 2000). For double color *in situ* hybridization, fluorescein-labeled probes

were prepared with fluorescein RNA labeling mix (Roche), and α-fluorescein alkaline phosphatase-conjugated antibody (Roche) was used.

RT-PCR

First-strand cDNA was generated from 1 μg of total RNA. PCR conditions were 94°C 10 s, 56°C 15 s, 72°C 30 s, 25 cycles. To detect both *z-mbx-S* and *z-mbx-L*, the following common primers were used: 5′-TTCACGCACTCACCCTGG-3′ and 5′-TGAACCATACCTGCACGC-3′, resulting in 222- and 237-bp fragments, respectively. To amplify *z-mbx-L* specifically, the following *z-mbx-L*-specific primers were used: 5′-TGGCTGTACATTTCAAG-3′ and 5′-TGAACCATACCTGCACGC-3′, resulting in a 206-bp fragment. The EF-1α primers were 5′-TGGGCACTCTACTTAAGGAC-3′ and 5′-TGTGGCAACAGGTGCAGTTC-3′.

Morpholino Oligonucleotide Injection

Both control and mbx morpholinos were obtained from Gene Tools, LLC, as follows: control-MO, 5′-CCTCTTACCTCAGTTACAATTTATA-3′; mbx-MO, 5′-ACTCCGTAGTGCTGCATGATTCACA-3′; mbx-MO2, 5′-TCAGTGAGTTCATGGCGTGGAGAGA-3′. Mbx-MO and mbx-MO2 are complementary to the zebrafish *mbx* mRNA sequence surrounding the initiation codon (underlined in mbx-MO) and the N-terminal domain from amino acids 10 to 18, respectively. Morpholinos were injected into the yolk region at the one- to four-cell stage as described previously (Kawahara and Dawid, 2001).

Detection of Apoptotic and Mitotic Cells

Dechorionated embryos were fixed in 4% paraformaldehyde (PFA) in phosphate-buffered saline (PBS). For detection of apoptotic cells, the TUNEL (terminal deoxynucleotidyl transferase-mediated dUTP nick-end labeling) assay (Cole and Ross, 2001) was performed as follows. The fixed embryos were washed with PBS three times for 15 min. Embryos were incubated overnight at room temperature with the labeling solution consisting of TdT (terminal deoxynucleotidyl transferase) and digoxigenin (DIG)–dUTP in TdT buffer (Invitrogen). Then, embryos were incubated with 1 mM EDTA in PBS at 65°C for 30 min and washed with PBS three times at room temperature for 15 min. Embryos were incubated overnight at 4°C with anti-DIG alkaline phosphatase (Roche) in blocking solution [0.1 M maleic acid (pH 7.5), 150 mM NaCl, 5% lamb serum, and 2% blocking reagent]. After washing six times with PBS (15 min each), apoptotic cells were detected by incubation with NBT (4-nitroblue tetrazolium chloride) and BCIP (5-bromo-4-chloroindolyl-phosphate) in the reaction buffer [100 mM Tris (pH 9.5), 50 mM $MgCl_2$, 100 mM NaCl, and 0.1% Tween 20].

For detection of mitotic cells, immunostaining with anti-phosphohistone H3 (Li *et al.*, 2000) was performed as follows. Fixed embryos were washed three times at room temperature with PBTw (1% Tween 20 in PBS) and then incubated with 10% lamb serum in PBTw. After washing twice with PBTw (30 min each), embryos were incubated with anti-phosphohistone H3 antibody in 10% lamb serum–PBTw overnight at 4°C. After washing four times with PBTw (30 min each), embryos were incubated with HRP-conjugated anti-IgG overnight at 4°C. After washing four times with PBTw (30 min each), mitotic cells were visualized by incubation with DAB in PBS containing 0.03% H_2O_2.

Lipophilic Dye Labeling of the Retinotectal Projection

As previously described (Fricke *et al.*, 2001), embryos were raised to 5 dpf by using phenylthiourea to inhibit melanin formation, fixed, and injected intraocularly with DiI, DiO, or DiD (Molecular Probes) in chloroform. In some cases, the brain was counterstained overnight with 0.5 μM SYTOX (Molecular Probes) after dissecting off the skin (Picker *et al.*, 1999). All eyes that were successfully injected and showed retinal axons exiting the eye were scored for projection phenotypes. Images were taken by confocal microscopy as previously described (Fricke *et al.*, 2001).

Cryostat Sections

Embryos were fixed overnight in 4% PFA and stored in MeOH. After rehydration, they were placed in 30% sucrose, embedded in OCT (Tissue-Tek), and cryosectioned at 12 μm. Sections were then double-labeled with the nuclear stain SYTOX and the RGC-specific monoclonal antibody zn-5/zn-8, originally generated by B. Trevarrow, and obtained from the Developmental Studies Hybridoma Bank (developed under auspices of the NICHD and maintained by the Department of Biological Sciences, University of Iowa). zn-5 and -8 are duplicate isolates of the same hybridoma (M. Westerfield, personal communication). Staining times were: overnight in zn-8 at 1:200, 4 h in Alexa 568 goat anti-mouse secondary antibody (Molecular Probes) at 1:400, and 10 min in 0.5 μM SYTOX (Molecular Probes); blocking solution was 5% goat serum and 0.25% Triton in PBS. Fluorescence images were taken with an Olympus Magnafire CCD camera, using the same exposures for experimental and control sections.

RESULTS

mbx Encodes a Novel Paired-Type Homeodomain Protein

We found partial nucleotide sequences representing a putative novel paired-type homeobox gene in the zebrafish EST database (GenBank Accession No. AI877798) and in the human genome sequence (chromosome 1). To study the molecular nature of this gene, we isolated its entire ORF from zebrafish and human cDNA libraries. We name this gene *midbrain homeobox* (*mbx*) according to its predominant early expression pattern, as presented below. As shown in Fig. 1A, zebrafish and human Mbx show high conservation in both N- and C-terminal domains (75% identity overall). In both species, we found two distinct splice variants producing long and short forms (*mbx-L* and *mbx-S*) that differ by only five amino acids within the conserved N terminus (Fig. 1A). Recently, our group and R. Behringer's group have independently isolated the mouse *mbx* gene (Miyamoto *et al.*, 2002; Ohtoshi *et al.*, 2002). The Mbx homeodomain is identical among zebrafish, mouse, and human and possesses some similarity to that of Aristaless and Pax family proteins (Fig. 1B; about 70% identity in the homeodomain). Aristaless and Pax contain glutamine and serine, respectively, at the critical position 50 in their homeodomains, whereas Mbx and Ptx have lysine residues at this position (ten Berge *et al.*, 1998). Indeed, the entire

Mbx protein is more similar to Ptx2 than to Cart1 and Alx4 (Fig. 1C). We failed to find a counterpart to Mbx in *Drosophila* genome sequences or an additional *mbx*-related gene in the human genome sequence. In addition, no conserved motif other than the homeodomain was detected in Mbx. Thus, sequence analysis indicates that Mbx is a novel homeoprotein highly conserved from zebrafish to human.

mbx Expression during Embryogenesis

Temporal and spatial expression of *mbx* in the early zebrafish embryo was examined by whole-mount *in situ* hybridization and RT-PCR analysis. Both analyses showed that *mbx* is not expressed up to midgastrula stages (Fig. 1D and data not shown), and is first transcribed in anterior neuroectoderm in the late gastrula (Fig. 2A). RT-PCR analysis indicates that both *mbx-S* and *mbx-L* are expressed at bud and 24-hpf stages (Fig. 1D). The initial *mbx* expression is refined to an oval ring with a midline gap (Fig. 2B, arrowhead) in the anterior neural plate at the bud stage. At this stage, *six3*, which is expressed in the prospective forebrain containing the future eye field (Kobayashi *et al.*, 1998), partly overlaps with the anterior *mbx* expression domain (Figs. 2B and 2C, dotted area), and a gap separates the posterior edge of the *mbx*-positive area from the future midbrain–hindbrain boundary (MHB) marked by *fgf8* (Fig. 2D). At the 1-somite stage, the edge of the anterior *mbx* domain abuts and appears to slightly overlap the *dlx3* expression domain (Figs. 2N–2P), placing this region in the presumptive forebrain. A particularly useful marker for the eye field and prospective tectum is *mab21l2*, which encodes a nuclear protein of unknown function (Kudoh and Dawid, 2001). At the 3-somite stage, expression in the posterior domain of *mab21l2* in the prospective tectal region is just beginning, while its expression in the eye field is already intense (Fig. 2R). At this stage, posterior *mbx* expression includes the *mab21l2* pretectal domain but extends over a larger area (Figs. 2Q–2S). We interpret this to mean that both genes are expressed in the prospective tectum, but *mab21l2* expression has not yet reached its full extent. This view is supported by the *mbx* pattern at the 5-somite stage, where the posterior domains of *mbx* and *mab21l2* are fully coincident (Figs. 2T–2V). It is also supported by the location of the posterior *mbx* domain at the 10-somite stage, which is completely included in the *otx2* domain that marks the midbrain and parts of the forebrain (Fig. 2E), and is located just anterior of the *pax2.1* expression domain (Figs. 2W–2Y). The conclusion that the major *mbx* expression domain in the midbrain corresponds to the prospective tectum is consistent with the predominant expression of *mbx* in the tectum at 26 hpf, forming a characteristic "heart" shape (Figs. 2F and 2G). Importantly, *mbx* is not expressed in the MHB through the first day of development (Figs. 2F and 2G, arrowhead).

The anterior *mbx* expression domain has become a faint oval by the 3- to 5-somite stage, extending to the apparent anterior edge of the neural plate (Figs. 2Q and 2T). Its lateral region appears to skirt the lateral edge of the eye field as visualized by *mab21l2* at the 3-somite stage and becomes included in the eye field by the 5-somite stage (Figs. 2Q–2S). These interpretations are supported by comparison of *mbx* and *pax2.1* expression at the 10-somite stage (Figs. 2W–2Y). The anterior expression of *mbx* gradually decreases during somitogenesis and has disappeared by 26 hpf (Fig. 2F). At this stage, a new area of *mbx* expression arises in a few hindbrain and spinal cord neurons. *mbx* expression in the hindbrain increases thereafter and has become intense in the rhombomeres and otic vesicle by 48 hpf; weak expression also arises in the diencephalon at this time (Figs. 2H and 2I). This pattern continues at 72 hpf, with additional staining seen in the retina (Figs. 2J–2M). Importantly, strong *mbx* expression in the tectum is maintained until 3 dpf.

Regulation of mbx Expression

In zebrafish, mutants in several pathways that regulate patterning of the early nervous system are available, allowing an investigation of their role in the control of *mbx* expression. Anterior–posterior (AP) patterning of the CNS is influenced by several signaling pathways, among them the Wnt pathway. The *headless* (*hdl*) mutant affects *tcf3* (Kim *et al.*, 2000), a gene encoding a transcription factor whose activity is modulated by the Wnt pathway. In *hdl* embryos, Wnt target genes are derepressed in the anterior neural plate, respecifying this region to assume more posterior characteristics (Kim *et al.*, 2000). In such mutants, *mbx* is expanded rostrally from the bud stage onward and extends to the anterior edge of the dorsal domain of the CNS at 26 hpf (Figs. 3B and 3C). Treatment with 0.3 M LiCl just after shield stage induces ectopic activation of the Wnt signaling pathway and results in defects in anterior brain formation (van de Water *et al.*, 2001). Anterior expansion of *mbx* was observed in LiCl-treated embryos as in *hdl* mutant embryos (Figs. 3D and 3E), suggesting that the Wnt pathway regulates the anterior limit of *mbx* expression. Next, we examined the expression of *mbx* in mutants that affect the MHB, as this region acts as an organizing center in patterning the surrounding areas of the developing brain. Both *no isthmus* (*noi/pax2.1*) and *acerebellar* (*ace/fgf8*) mutants lack the MHB constriction (Lun and Brand, 1998; Reifers *et al.*, 1998). Although *pax2.1*, *fgf8*, and *wnt1* genes are activated independently in the future MHB, these pathways become mutually dependent during maintenance stages (Rhinn and Brand, 2001). Further, two mutants differ in that the formation of the tectum is strongly affected in *noi* but not in *ace*. In *noi* mutant embryos, *mbx* expression is partly diminished at the 10-somite stage (Figs. 3F and 3G), and at 24 hpf continues to be reduced in the midbrain area but extends caudally beyond its normal expression limit (Fig. 3I, white arrowhead). In *ace* mutant embryos, which retain a tectum, *mbx* expression is not affected at the 10-somite stage (data not shown), while at 24 hpf, *mbx* expression in

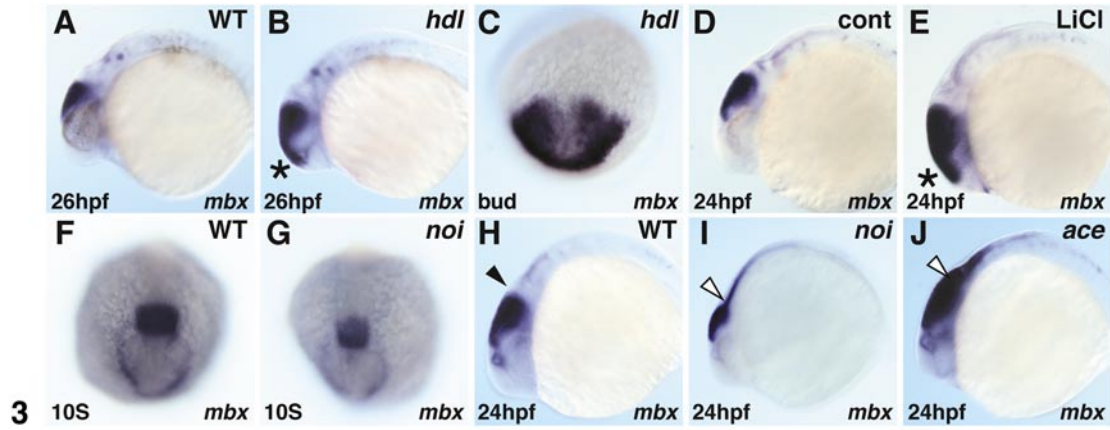

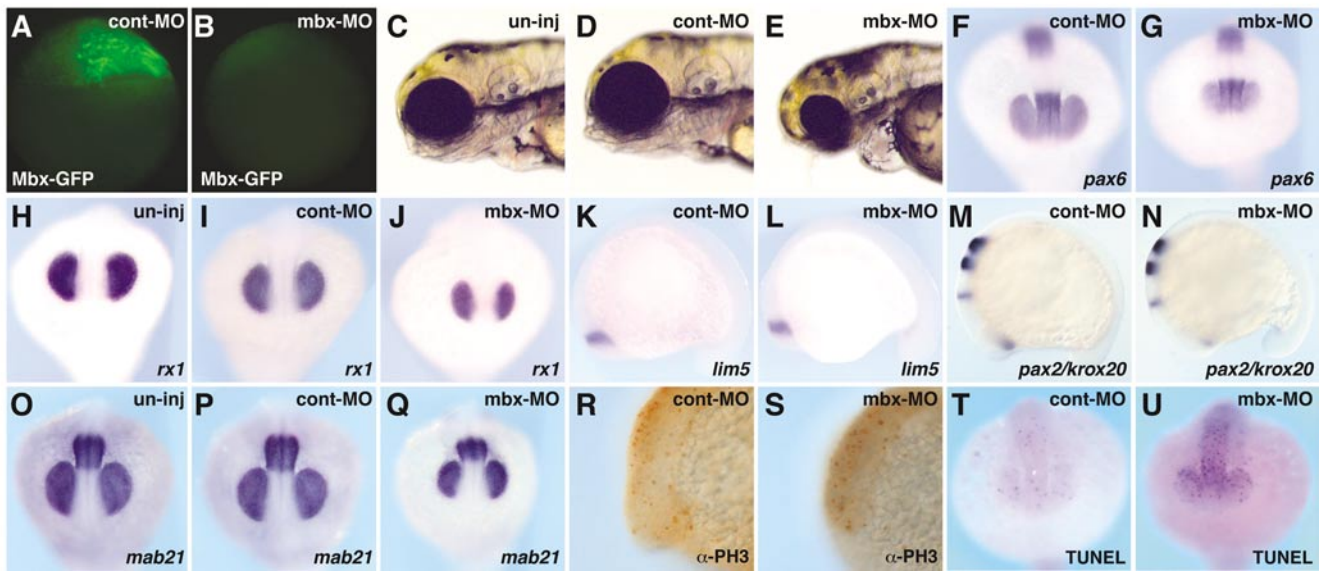

FIG. 3. *mbx* expression in mutant embryos. Whole-mount *in situ* hybridization of *mbx*. Black and white arrowheads indicate the MHB and putative MHB region, respectively. In *headless* (*hdl*) mutants, *mbx* expression is expanded rostrally at bud and 26-hpf stages (B, C). Similarly, anterior *mbx* expansion at 24 hpf is observed in embryos treated with 0.3 M LiCl just after shield stage (E). In the *no isthmus*^{tu29a} (*noi)* mutant, *mbx* expression is slightly diminished at the 10-somite stage (G), and reduced in intensity but expanded caudally at 24 hpf (I). In the *acerebellar*^{ti282a} (*ace)* mutant, *mbx* expression in the tectum is retained and again expanded caudally (J).

FIG. 4. *mbx* knockdown phenotype with morpholino oligonucleotides. (C, H, O) Uninjected embryos; (A, D, F, I, K, M, P, R, T) cont-MO (5 ng)-injected embryos; (B, E, G, J, L, N, Q, S, U) mbx-MO (5 ng)-injected embryos. (A, B) Mbx-GFP expression at the sphere stage; lateral view. Mbx-GFP RNA (0.5 ng) was injected into the blastomere at the one-cell stage and either mbx-MO or cont-MO was injected into the yolk region. Mbx-GFP expression was suppressed in mbx-MO-injected embryos (B), but not in cont-MO-injected embryos (A). (C–E) Live embryos at 3 dpf: lateral view. Injection of mbx-MO, but not cont-MO, led to a reduction of eye size. (F–Q) Whole-mount *in situ* hybridization with probes shown at the bottom of each panel at the 15-somite stage. (F–J, O–Q) Anterior view. (K–N) Lateral view. Mbx-MO injection led to a smaller eye field visualized with *rx1, mab21l2* and *pax6* (F–J, O–Q), and a smaller tectal domain visualized by *mab21l2* (O–Q). Expression of *pax6* and *lim5* (diencephalon: F, G, K, L), *pax2.1* (optic stalk and MHB: M, N), and *krox20* (hindbrain: M, N) are similar in cont-MO- and mbx-MO-injected embryos. (R, S) Anti-phosphohistone H3 antibody, visualizing mitotic cells, stains similar numbers of cells in cont-MO- and mbx-MO-injected embryos. (T, U) TUNEL assay indicates an increased number of apoptotic cells in mbx-MO-injected embryos.

the tectum is retained and again expands caudally into the hindbrain (Fig. 3J, white arrowhead). These results indicate that the MHB constitutes a boundary that restricts posterior expression of *mbx* during somitogenesis stages.

Functional Analysis of mbx

The expression pattern of *mbx* suggests a role for this gene in the development of the mid and forebrain. To test

TABLE 1

Effects of mbx-MO on the Size of Selected Brain Regions

	Size relative to uninjected embryos (%)			
	Eye	Tectum	r2	r4
Uninjected	100.0 ± 4.1	100.0 ± 3.8	100.0 ± 6.5	100.0 ± 3.7
cont-MO	100.8 ± 2.5	99.5 ± 4.4	99.8 ± 6.7	97.2 ± 8.9
mbx-MO	58.3 ± 5.1*	71.1 ± 5.3*	91.2 ± 8.8	98.5 ± 9.5

Note. Embryos were injected with the indicated morpholinos (5 ng) at the two- to four-cell stage. The tectum and rhombomeres were visualized at 3 dpf by *in situ* hybridization with *mbx*. The diameter of the eye, the diagonal width of the right tectum, and the width of rhombomeres 2 and 4 (r2 and r4) were measured. The average of 10 embryos is expressed as a percentage of uninjected controls, mean ± SD.

* $P < 0.001$, comparing mbx-MO to cont-MO by Student's *t* test.

this possibility, we analyzed the phenotype generated by reducing *mbx* function with the aid of morpholino-based antisense oligonucleotides. We designed mbx-morpholinos (mbx-MO) with a sequence complementary to the N-terminal domain around the initiation codon of both *mbx-L* and *mbx-S*, while a control-morpholino (cont-MO) has an unrelated sequence. To test the effect of the mbx-MO, we injected synthetic mRNA (0.5 ng) for a Mbx-GFP fusion into one-cell stage embryos, and subsequently injected either mbx-MO (5 ng) or cont-MO (5 ng) into the yolk. Expression of Mbx-GFP in the blastoderm was strongly suppressed by injection of mbx-MO but not of cont-MO (Figs. 4A and 4B). Embryos injected with 5 ng mbx-MO or cont-MO into the yolk region at the one- to four-cell stage showed essentially normal overall morphology of the trunk and tail (data not shown). In contrast, injection of mbx-MO affects anterior brain development, showing a small eye phenotype at 3 dpf (91%, $n = 34$), while control-MO-injected embryos were unaffected (small eye: 2%, $n = 50$) (Figs. 4C–4E). In addition, we observed jaw defects and

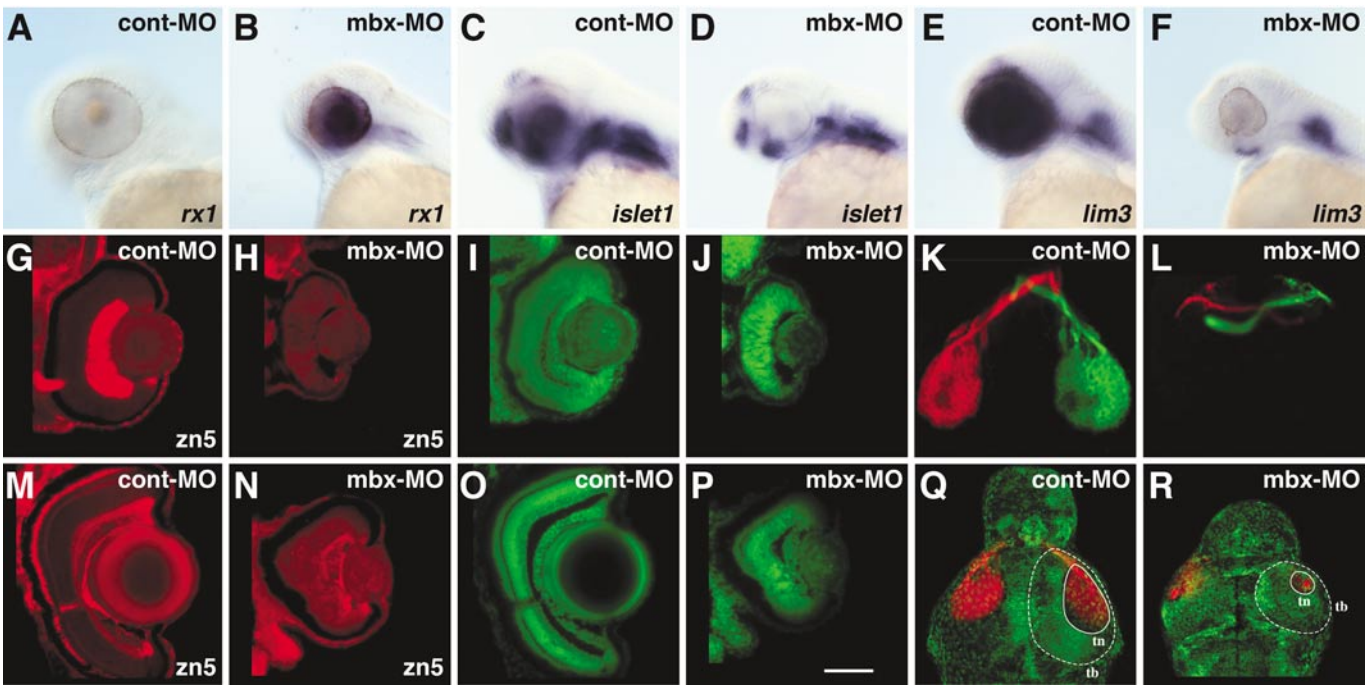

FIG. 5. Visual system phenotype in mbx-MO-injected embryos. (A–D) Expression patterns of retinal markers at 48 hpf. The expression of *rx1* in retina is down-regulated in cont-MO-injected (A), but retained in mbx-MO-injected embryos (B). *Islet1* and *lim3* are activated in the retina of cont-MO-injected (C, E) but not mbx-MO-injected embryos (D, F); in contrast, expression of both genes in the hindbrain is not affected (D, F). (G–J, M–P) Retinal phenotype at 48 hpf (G–J) and 5 dpf (M–P). The number of RGCs and retinal axons, as visualized by zn-5 immunostaining, is greatly reduced in mbx-MO-injected embryos (H, N) compared with controls (G, M). (G) and (H) are shown at the same brightness setting to illustrate the absence of signal in (H). Nuclear staining using SYTOX (green) shows that retinal lamination is disorganized in mbx-MO-injected embryos (I, J, O, P). (K, L, Q, R) Retinotectal projections at 5 dpf. For clarity, the labeled eyes have been digitally removed. (K, L) The right and left eyes were labeled with diI (red) and diO (green), respectively. The number of retinal axons is greatly reduced in mbx-MO-injected embryos (L), but the remaining axons project normally to the contralateral side. (Q, R) Both eyes were labeled with diD (red), and the embryo was stained with SYTOX (green), which outlines the tectal border (tb) but does not label the cell-sparse tectal neuropil (tn). The size of the tecta, and especially the neuropil, was reduced in mbx-MO-injected embryos (R).

heart edema (96%, $n = 80$) in these embryos (Figs. 4C–4E); heart edema is also observed in the *noi* mutant (Brand *et al.*, 1996). A similar small eye phenotype was observed in embryos injected with a different oligonucleotide, mbx-MO2 (data not shown). The specificity of the effects of mbx morpholinos is further supported by the fact that several additional morpholinos, designed against different neural-specific genes, failed to elicit a small eye phenotype (data not shown). For quantitative evaluation, we chose to compare eye diameter and tectal width with the width of rhombomeres in mbx-MO-injected embryos. As described in Table 1, we found substantial reduction in the size of eyes and tectum, whereas the rhombomeres were unaffected by the antisense reagent.

To characterize the molecular events underlying the small eye phenotype, we investigated the expression of neural markers in mbx-MO-injected embryos. As shown in Fig. 4, *rx1* (eye marker) and *mab21l2* (eye and tectum marker) are expressed at essentially correct positions but in smaller fields in mbx-MO-injected embryos (Figs. 4H–4J and 4O–4Q). Similarly, the *pax6* expression domain in the eye field is significantly smaller in the mbx-MO-injected embryos (Figs. 4F and 4G). These results are consistent with the small eye phenotype at 3 dpf. In contrast, *pax6* and *lim5* expression in the diencephalon between the eyes is maintained (Figs. 4F, 4G, 4K, and 4L), and the position and intensity of several other brain markers (*otx2*, *dlx3*, *pax2.1*, *fgf8*, *krox20*, *zath1*, *islet1*, *fkd6*) are quite similar in control-MO- and mbx-MO-injected embryos (Figs. 4M and 4N; and data not shown). Although tectum size in the mbx-MO-injected embryos is diminished at 26 h as it is earlier, *mab21l2* is still expressed in the tectum of mbx-MO-injected embryos at this stage (data not shown).

Reduction in the size of eyes and tectum could result from effects of *mbx* depletion on cell proliferation or cell death. Mitotic cells in the anterior brain, as visualized by anti-phosphohistone H3 antibody that stains cells in late G_2 and M phase (Li *et al.*, 2000), were comparable in uninjected, cont-MO-injected, and mbx-MO-injected embryos (Figs. 4R and 4S; and data not shown). In contrast, the number of apoptotic cells judged by TUNEL assay (Cole and Ross, 2001) was substantially higher in mbx-MO-injected embryos as compared with uninjected and cont-MO-injected embryos (Figs. 4T and 4U; and data not shown). The reduction of *mbx* expression thus leads to an increased level of cell death in the anterior brain by the 24-hpf stage.

mbx Function in the Visual System

The *mbx* expression pattern and mbx-morpholino knockdown phenotype suggest that this gene is involved in the development of the eye and tectum. Retinal axons start to exit from the eye at 36 hpf and reach their appropriate tectal targets by 48 hpf (Burrill and Easter, 1994); the retina undergoes extensive differentiation during the first several days of development. Therefore, we tested whether depletion of Mbx affected eye development between 2 and 5 dpf. First, we examined the expression of retinal markers at 48 hpf. When the neural retina begins to differentiate, *islet1* and *lim3* are induced in the eye (Masai *et al.*, 2000), while *rx1* expression is down-regulated (Chuang *et al.*, 1999). As previously reported, *rx1* expression has disappeared by 48 hpf in uninjected and cont-MO-injected embryos, whereas *rx1* expression in mbx-MO-injected embryos was maintained (Figs. 5A and 5B; and data not shown). Likewise, expression of *islet1* and *lim3* was seen in the eyes of uninjected and cont-MO-injected embryos but not in the eyes of mbx-MO-injected embryos, while hindbrain expression of both genes was unaffected (Figs. 5C–5F). In addition, the formation of the retinal ganglion cell (RGC) layer, as judged by immunostaining with zn-5, was severely affected in mbx-MO-injected embryos at 48 hpf and 5 dpf (Figs. 5G, 5H, 5M, and 5N). Concomitantly, retinal lamination was disorganized in the mbx-MO-injected embryos at 48 hpf, and maturation seemed to progress only slightly between 2 and 5 dpf, while extensive lamination occurs in control eyes during this period (Figs. 5I, 5J, 5O, and 5P). We examined further whether depletion of Mbx affected the functional connections between the eye and the tectum by labeling retinal axons with lipophilic dye injections at 5 dpf, when the retinotectal projections are normally mature (Burrill and Easter, 1994). The number of retinal axons was greatly reduced in mbx-MO-injected embryos, consistent with the small size of the eyes (100%, $n = 17$ labeled eyes). The relatively few optic axons that remained navigated across the optic chiasm in a normal manner, projecting to the contralateral tectum (Figs. 5K and 5L) in both control (100%, $n = 18$) and mbx-MO-injected embryos (100%, $n = 25$). Counterstaining the brain with the nuclear stain SYTOX (Picker *et al.*, 1999) showed that mbx-MO tecta had disproportionately tiny neuropils, presumably as a result of the small number of retinal axons (Figs. 5Q and 5R). Thus, these results indicate that *mbx* is required for the formation of normal-sized eyes, for tectum and eye maturation including specification of the normal number of retinal axons, and for lamination of the retina, but not for pathfinding between the eyes and the tectum.

Mbx Appears to Act As a Repressor

The role of Mbx was also tested by overexpression studies of the wild type molecule and by expression of chimeric molecules with predictable properties in the embryo. Injection of *mbx-L* mRNA into one-cell stage zebrafish embryos led to a general dorsalized phenotype with elongated shape at bud stage (data not shown). A similar phenotype was seen after injection of ENG-mbx, in which the Mbx homeodomain is fused to the *Drosophila* Engrailed repressor domain (data not shown). We believe that this dorsalization is a nonspecific consequence of widespread Mbx or ENG-mbx overexpression. In contrast, injection of VP16-mbx, a fusion of the Mbx homeodomain to the VP16 activation domain of herpes simplex virus I, caused a small eye phenotype and a decrease of *rx1* and *mab21l2* expression, but did not affect

the expression of *otx2* (Fig. 6). These phenotypes are similar to those resulting from injection of mbx-MO, and this concurrence suggests that VP16-mbx interferes with the function of the endogenous Mbx protein. As the activating form of Mbx, VP16-mbx, appears to behave as an antimorph, we suggest that Mbx acts as a transcriptional repressor in the embryo, and we further conclude that reduction in the size of eyes and tectum is the loss-of-function phenotype of the *mbx* gene.

DISCUSSION

In this paper, we describe the isolation and characterization of a homeobox gene, *mbx*, which is expressed in the anterior neural ectoderm during early neurogenesis. The initial *mbx* expression domain ranges from the anterior edge of the neural plate to the presumptive midbrain region. Expression of *mbx* at the anterior edge of the neuroectoderm gradually decreases during early somitogenesis, while expression is maintained in the presumptive midbrain where it intensifies and becomes restricted to the prospective tectal region. Among homeobox genes, *mbx* is unique in being largely restricted to the tectum from mid somitogenesis stages to 26 hpf, but at later stages, this gene expands its domain to the diencephalon and hindbrain. Mbx is highly conserved between zebrafish, mouse, and human, and the expression pattern in the mouse is also similar to that described here for zebrafish, being predominant in the midbrain at early stages and expanding subsequently to both forebrain and hindbrain (Miyamoto *et al.*, 2002; Ohtoshi *et al.*, 2002).

Comparing the *mbx* pattern to that of other early brain markers, we note that *pax7* expression starts in the presumptive midbrain around the 8-somite stage, but quickly spreads to a wide brain area including parts of the diencephalon, tectum, and hindbrain before the 14-somite stage (Seo *et al.*, 1998). The *eng1,2* and *pax2,5* genes are expressed in different regions of the brain at early stages, predominating in the MHB by 26 hpf. Thus it appears that *mbx* is the first known homeobox gene that is expressed predominantly in the presumptive tectum from the end of gastrulation through the first day of zebrafish development.

Regulation of mbx Expression in the Anterior Neuroectoderm

Like other neural genes, *mbx* is sensitive to the level of BMP signaling, being reduced in *chordino/chordin* and expanded in *swirl/bmp2b* mutant embryos (data not shown). Further, the Wnt signaling pathway, which affects AP patterning in the neuroectoderm, plays a role in delimiting the rostral boundary of the *mbx* domain as this domain is expanded in *hdl/tcf3* mutant and late LiCl-treated embryos, both of which exhibit posterior transformation of the anterior neural plate (Kim *et al.*, 2000; van de Water *et al.*, 2001). The posterior boundary of the *mbx* domain is formed by the isthmus at the MHB, a region known to have organizer activity in regulating the pattern of surrounding regions of the developing brain. In the *ace/fgf8* and *noi/pax2.1* mutants, both of which lack the MHB (Lun and Brand, 1998; Reifers *et al.*, 1998), *mbx* expression is expanded caudally, implicating the MHB in establishing the posterior border of the *mbx* domain and thereby restricting *mbx* expression to the midbrain.

Function of mbx in the Anterior Neuroectoderm

Functional studies that include interference with expression through morpholino antisense oligonucleotides and expression of VP16-mbx, a putative dominant negative construct, indicate that *mbx* has a role in the development of the anterior neural plate. A major consequence of injection of mbx-MO or of VP16-mbx was a reduction in the size of the eyes and tectum without substantial changes in other regions of the brain (see Table 1). This was associated with smaller domains of *rx1*, *pax6*, and *mab21l2* expression in the eye field and the tectum anlage. In contrast, similar expression patterns were observed in cont-MO- and mbx-MO-injected embryos for marker genes in other CNS regions, including the forebrain (*six3*, *lim5*), olfactory placode (*dlx3*), optic stalk (*pax2.1*), neural crest (*fkd6*), and hindbrain (*krox20*, *zath1*). The mbx-MO-induced phenotype may be due to a requirement for early expression of *mbx* in the eye field and tectum to achieve balance between cell proliferation and apoptotic cell death in the developing anterior brain. While proliferation seemed unaffected, we observed an increase in the number of apoptotic cells in the anterior brain of mbx-MO-injected embryos.

During neuronal differentiation of the retina starting at about 30 hpf, the *islet1* and *lim3* genes are activated (Masai *et al.*, 2000), while *rx1* is down-regulated (Chuang *et al.*, 1999). Both activation of *islet1* and *lim3* and suppression of *rx1* failed to occur in the retina of mbx-MO-injected embryos. These events do not represent a general delay of development as *islet1* and *lim3* expression in the hindbrain was unaffected. These results suggest that *mbx* is required for proper maturation of the retina. The lamination of the retina was disorganized in mbx-MO-injected embryos and the number of retinal axons was greatly reduced, although the remaining axons navigated correctly to the contralateral tectum. While the mbx-MO phenotype is reminiscent of zebrafish retinotectal mutants with small tecta (including *noi*), in which retinal axons project and arborize normally to form a miniature topographic map (Trowe *et al.*, 1996), the tectal neuropil in mbx-MO-injected embryos is significantly smaller than was found in these mutants. In summary, we propose that *mbx*, a novel paired-type homeodomain protein, is required for size regulation and proper maturation of the retina, and has a second role in the regulation of tectal size.

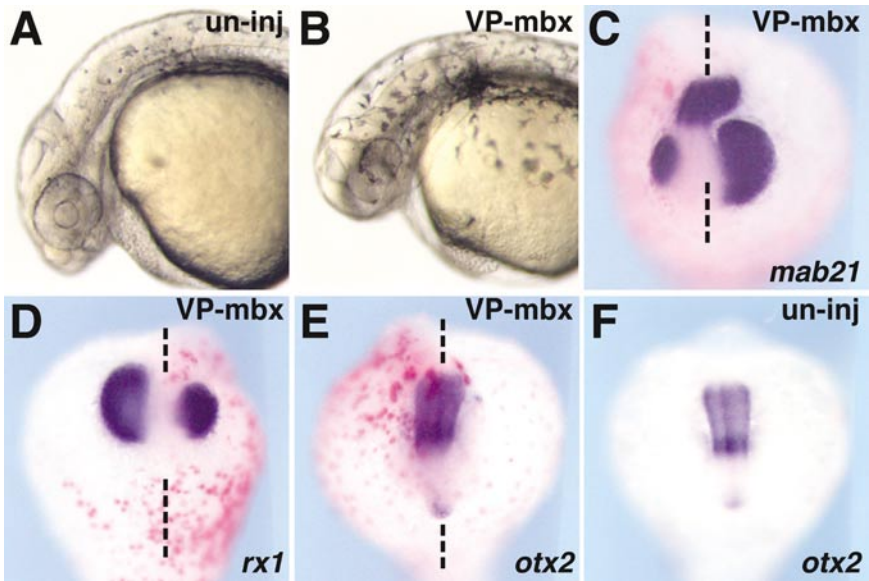

FIG. 6. VP16-mbx expression inhibits eye and tectum formation. VP16-mbx mRNA (10 pg) together with β-galactosidase mRNA (300 pg), was injected into 1- to 2-cell-stage zebrafish embryos. (A, B) Live embryos at 25 hpf; injection of VP16-mbx caused a small eye phenotype (B). (C–F) *In situ* hybridization with *mab21l2* (C), *rx1* (D), and *otx2* (E, F) at the 15-somite stage. Both *mab21l2* and *rx1* (purple staining) expression are smaller on the side that received the VP16-mbx mRNA injection (C, D), while *otx2* expression is not affected (E). Red staining indicates the β-gal injection tracer.

ACKNOWLEDGMENTS

We thank M. Tsang, L. Nathan, and A. Chitnis for zebrafish mutants and reagents, E. Laver for assistance, A. Kugath for expert help with cryostat sectioning, and A. Chitnis and C. Kimmel for critical comments.

REFERENCES

Andreazzoli, M., Gestri, G., Angeloni, D., Menna, E., and Barsacchi, G. (1999). Role of Xrx1 in Xenopus eye and anterior brain development. *Development* **126,** 2451–2460.

Appel, B. (2000). Zebrafish neural induction and patterning. *Dev. Dyn.* **219,** 155–168.

Arakawa, H., Nakamura, T., Zhadanov, A. B., Fidanza, V., Yano, T., Bullrich, F., Shimizu, M., Blechman, J., Mazo, A., Canaani, E., and Croce, C. M. (1998). Identification and characterization of the ARP1 gene, a target for the human acute leukemia ALL1 gene. *Proc. Natl. Acad. Sci. USA* **95,** 4573–4578.

Brand, M., Heisenberg, C. P., Jiang, Y. J., Beuchle, D., Lun, K., Furutani-Seiki, M., Granato, M., Haffter, P., Hammerschmidt, M., Kane, D. A., Kelsh, R. N., Mullins, M. C., Odenthal, J., van Eeden, F. J., and Nusslein-Volhard, C. (1996). Mutations in zebrafish genes affecting the formation of the boundary between midbrain and hindbrain. *Development* **123,** 179–190.

Burrill, J. D., and Easter, S. S., Jr. (1994). Development of the retinofugal projections in the embryonic and larval zebrafish (*Brachydanio rerio*). *J. Comp. Neurol.* **346,** 583–600.

Chuang, J. C., Mathers, P. H., and Raymond, P. A. (1999). Expression of three Rx homeobox genes in embryonic and adult zebrafish. *Mech. Dev.* **84,** 195–198.

Chuang, J. C., and Raymond, P. A. (2001). Zebrafish genes rx1 and rx2 help define the region of forebrain that gives rise to retina. *Dev. Biol.* **231,** 13–30.

Cole, L. K., and Ross, L. S. (2001). Apoptosis in the developing zebrafish embryo. *Dev. Biol.* **240,** 123–142.

Fricke, C., Lee, J. S., Geiger-Rudolph, S., Bonhoeffer, F., and Chien, C. B. (2001). astray, a zebrafish roundabout homolog required for retinal axon guidance. *Science* **292,** 507–510.

Goulding, M. D., Chalepakis, G., Deutsch, U., Erselius, J. R., and Gruss, P. (1991). Pax-3, a novel murine DNA binding protein expressed during early neurogenesis. *EMBO J.* **10,** 1135–1147.

Jostes, B., Walther, C., and Gruss, P. (1990). The murine paired box gene, Pax7, is expressed specifically during the development of the nervous and muscular system. *Mech. Dev.* **33,** 27–37.

Kawahara, A., and Dawid, I. B. (2001). Critical role of biklf in erythroid cell differentiation in zebrafish. *Curr. Biol.* **11,** 1353–1357.

Kawahara, A., Wilm, T., Solnica-Krezel, L., and Dawid, I. B. (2000). Antagonistic role of vega1 and bozozok/dharma homeobox genes in organizer formation. *Proc. Natl. Acad. Sci. USA* **97,** 12121–12126.

Kim, C. H., Oda, T., Itoh, M., Jiang, D., Artinger, K. B., Chandrasekharappa, S. C., Driever, W., and Chitnis, A. B. (2000). Repressor activity of Headless/Tcf3 is essential for vertebrate head formation. *Nature* **407,** 913–916.

Kobayashi, M., Toyama, R., Takeda, H., Dawid, I. B., and Kawakami, K. (1998). Overexpression of the forebrain-specific homeobox gene six3 induces rostral forebrain enlargement in zebrafish. *Development* **125,** 2973–2982.

Kudoh, T., and Dawid, I. B. (2001). Zebrafish mab21l2 is specifically expressed in the presumptive eye and tectum from early somitogenesis onwards. *Mech. Dev.* **109,** 95–98.

Li, Z., Hu, M., Ochocinska, M. J., Joseph, N. M., and Easter, S. S., Jr. (2000). Modulation of cell proliferation in the embryonic retina of zebrafish (*Danio rerio*). *Dev. Dyn.* **219,** 391–401.

Lun, K., and Brand, M. (1998). A series of no isthmus (noi) alleles of the zebrafish pax2.1 gene reveals multiple signaling events in development of the midbrain–hindbrain boundary. *Development* **125,** 3049–3062.

Mansouri, A., and Gruss, P. (1998). Pax3 and Pax7 are expressed in commissural neurons and restrict ventral neuronal identity in the spinal cord. *Mech. Dev.* **78,** 171–178.

Masai, I., Stemple, D. L., Okamoto, H., and Wilson, S. W. (2000). Midline signals regulate retinal neurogenesis in zebrafish. *Neuron* **27,** 251–263.

Mathers, P. H., Grinberg, A., Mahon, K. A., and Jamrich, M. (1997). The Rx homeobox gene is essential for vertebrate eye development. *Nature* **387,** 603–607.

Matsunaga, E., Araki, I., and Nakamura, H. (2001). Role of Pax3/7 in the tectum regionalization. *Development* **128,** 4069–4077.

Miyamoto, T., Kawahara, A., Teufel, A., Mukhopadhyay, Y, Zhao, M., Dawid, I. B., and Westphal, H. (2002). Mbx, a novel mouse homeobox gene. *Dev. Genes Evol.* **212,** 104–106.

Ohtoshi, A., Nishijima, I., Justice, M. J., and Behringer, R. R. (2002) Dmbx1,. a novel evolutionarily conserved paired-like homeobox gene expressed in the brain of mouse embryos. *Mech. Dev.* **110,** 241–244.

Picker, A., Brennan, C., Reifers, F., Clarke, J. D., Holder, N., and Brand, M. (1999). Requirement for the zebrafish mid-hindbrain boundary in midbrain polarisation, mapping and confinement of the retinotectal projection. *Development* **126,** 2967–2978.

Puschel, A. W., Gruss, P., and Westerfield, M. (1992). Sequence and expression pattern of pax-6 are highly conserved between zebrafish and mice. *Development* **114,** 643–651.

Qu, S., Li, L., and Wisdom, R. (1997). Alx-4: cDNA cloning and characterization of a novel paired-type homeodomain protein. *Gene* **203,** 217–223.

Quiring, R., Walldorf, U., Kloter, U., and Gehring, W. J. (1994). Homology of the eyeless gene of Drosophila to the Small eye gene in mice and Aniridia in humans. *Science* **265,** 785–789.

Reifers, F., Bohli, H., Walsh, E. C., Crossley, P. H., Stainier, D. Y., and Brand, M. (1998). Fgf8 is mutated in zebrafish acerebellar (ace) mutants and is required for maintenance of midbrain–hindbrain boundary development and somitogenesis. *Development* **125,** 2381–2395.

Rhinn, M., and Brand, M. (2001). The midbrain–hindbrain boundary organizer. *Curr. Opin. Neurobiol.* **11,** 34–42.

Rubenstein, J. L., Shimamura, K., Martinez, S., and Puelles, L. (1998). Regionalization of the prosencephalic neural plate. *Annu. Rev. Neurosci.* **21,** 445–477.

Schwarz, M., Alvarez-Bolado, G., Urbanek, P., Busslinger, M., and Gruss, P. (1997). Conserved biological function between Pax-2 and Pax-5 in midbrain and cerebellum development: evidence from targeted mutations. *Proc. Natl. Acad. Sci. USA* **94,** 14518–14523.

Seo, H. C., Saetre, B. O., Havik, B., Ellingsen, S., and Fjose, A. (1998). The zebrafish Pax3 and Pax7 homologues are highly conserved, encode multiple isoforms and show dynamic segment-like expression in the developing brain. *Mech. Dev.* **70,** 49–63.

ten Berge, D., Brouwer, A., el Bahi, S., Guenet, J. L., Robert, B., and Meijlink, F. (1998). Mouse Alx3: An aristaless-like homeobox gene expressed during embryogenesis in ectomesenchyme and lateral plate mesoderm. *Dev. Biol.* **199,** 11–25.

Ton, C. C., Miwa, H., and Saunders, G. F. (1992). Small eye (Sey): Cloning and characterization of the murine homolog of the human aniridia gene. *Genomics* **13,** 251–256.

Trowe, T., Klostermann, S., Baier, H., Granato, M., Crawford, A. D., Grunewald, B., Hoffmann, H., Karlstrom, R. O., Meyer, S. U., Muller, B., Richter, S., Nusslein-Volhard, C., and Bonhoeffer, F. (1996). Mutations disrupting the ordering and topographic mapping of axons in the retinotectal projection of the zebrafish, *Danio rerio*. *Development* **123,** 439–450.

Urbanek, P., Fetka, I., Meisler, M. H., and Busslinger, M. (1997). Cooperation of Pax2 and Pax5 in midbrain and cerebellum development. *Proc. Natl. Acad. Sci. USA* **94,** 5703–5708.

van de Water, S., van de Wetering, M., Joore, J., Esseling, J., Bink, R., Clevers, H., and Zivkovic, D. (2001). Ectopic Wnt signal determines the eyeless phenotype of zebrafish masterblind mutant. *Development* **128,** 3877–3888.

Walther, C., Guenet, J. L., Simon, D., Deutsch, U., Jostes, B., Goulding, M. D., Plachov, D., Balling, R., and Gruss, P. (1991). Pax: A murine multigene family of paired box-containing genes. *Genomics* **11,** 424–434.

Wurst, W., Auerbach, A. B., and Joyner, A. L. (1994). Multiple developmental defects in Engrailed-1 mutant mice: An early mid-hindbrain deletion and patterning defects in forelimbs and sternum. *Development* **120,** 2065–2075.

Wurst, W., and Bally-Cuif, L. (2001). Neural plate patterning: Upstream and downstream of the isthmic organizer. *Nat. Rev. Neurosci.* **2,** 99–108.

Zhang, L., Mathers, P. H., and Jamrich, M. (2000). Function of Rx, but not Pax6, is essential for the formation of retinal progenitor cells in mice. *Genesis* **28,** 135–142.

Zhao, G. Q., Zhou, X., Eberspaecher, H., Solursh, M., and de Crombrugghe, B. (1993). Cartilage homeoprotein 1, a homeoprotein selectively expressed in chondrocytes. *Proc. Natl. Acad. Sci. USA* **90,** 8633–8637.

Received for publication January 2, 2002
Revised April 15, 2002
Accepted April 19, 2002
Published online June 14, 2002